11 WCEE
Copyright © 1996 Elsevier Science Ltd
Paper No. 1215. (quote when citing this article)
Eleventh World Conference on Earthquake Engineering
ISBN: 0 08 042822 3

STRUCTURAL DESIGN CHARTS AND EQUATIONS OF DEFORMATION CAPACITY OF REINFORCED CONCRETE COLUMNS AFTER FLEXURAL YIELDING

EIICHI INAI [1] and HISAHIRO HIRAISHI [2]

1 Structural Engineering Division, Technical Research Institute, Hazama Corporation, Karima-nishimukai 515-1, Tsukuba, Ibaraki, 305, Japan
2 Structural Engineering Department, Building Research Institute, Ministry of Construction, Tatehara 1, Tsukuba, Ibaraki, 305, Japan

ABSTRACT

Reinforced concrete columns subjected to shear and high axial forces typically fail due to crush of concrete after flexural yielding. Many of studies on the evaluation of ductility of these columns have been performed by various researchers. Most of them were statistical studies based on experimental results, but an appropriate design equation for practical use has not yet been proposed. Some of the researchers carried out a theoretical investigation assuming a certain limit of either compressive or tensile strain at the critical section, but the correlations between theoretical and experimental results were inadequate, and they did not describe ductility of members but only that of the critical sections.

This paper describes the theoretical deformation capacity of columns under monotonically increasing loading or cyclic loading, design charts and equations for the deformation capacity of columns are presented. The results were compared to experimental results, and an excellent agreement was achieved.

KEYWORDS

Reinforced concrete columns; deformation capacity; flexural yielding; high axial load; monotonically increasing lateral loading; cyclic lateral loading.

INTRODUCTION

The deformation capacity is one of the most important factors in evaluating the seismic performance of structural members. However, a reasonable definition has not yet been proposed. The deformation at the deterioration in strength of 80% of the ultimate is often taken as the deformation capacity in the experimental results, but the reason for this is not clear physically. Some researchers discussed a critical strain in the extreme compressive concrete fiber or a critical tension strain in steel bars at the critical section (Suzuki *et al.*, 1988, Koyanagi *et al.*, 1988). However, the relation between the capacity at the sections and that in the members was not explained. The authors, based on the experimental results of columns, showed that a critical point in the vertical stretching of the tension side in the hinge region existed when columns were subjected to monotonically increasing lateral load, and that the mechanism of energy absorption in a whole column changed dramatically at this critical point (Hiraishi *et al.*, 1990a). This point is referred to as the stable limit under monotonically increasing loading. The drift angle of columns at this stable limit can be calculated based on the strains and curvature at the critical section. The validity of the calculation method has been examined (Hiraishi *et al.*, 1990b and Inai *et al.*, 1992).

During cyclic lateral loading with a deformation amplitude, the edge zone at the critical section of columns may be subjected to inelastic compressive strains or tensile strains at the peak deformation, but the central zone at the critical section may still be in the elastic state and sustain most of the axial load. When the deformation amplitude exceeds a certain magnitude, the central zone cannot remain elastic any longer. This results in an accumulative axial shortening in the columns due to the hysteresis characteristics of the concrete itself, and the lateral load carrying capacity successively deteriorates at each cycle in case that the stress versus strain curve of concrete has a descending slope after the maximum strength. This means that this deformation amplitude in cyclic loading which causes inelastic stain over a whole critical section is also the deformation capacity of columns (Hiraishi *et al.*, 1993). As a result, the deformation capacity when subjected to cyclic loading is given by the smaller deformation of the two deformations: one defined by the stable limit and the other defined by the hysteresis behavior of concrete under cyclic loading. In this paper, design charts and equations for deformation capacity derived from the theoretical results mentioned above are presented, and an excellent correlation between the equation and experimental results is shown.

DEFORMATION CAPACITY DEFINED BY MONOTONICALLY INCREASING LOADING

The drift angle of columns at the stable limit is calculated based on the strains and curvature at the critical section. The strains and curvature at the stable limit under the assumption of the perfect elasto-plastic relation for steel is derived as follows (see Fig. 1 and Fig. 2). This solution is shown in Suzuki *et al.*, 1988 and Koyanagi *et al.*, 1988. The solution taking account of strain hardening in both tension and compression steel bars is shown in Hiraishi *et al.*, 1990a.

The maximum strain in tensile steel bars at the stable limit:

$$\varepsilon_{O,MAX} = \underline{(S_3 - S_1)/(S_1 + S_2)} \cdot \varepsilon_{C,CR} \tag{1}$$

The curvature at the stable limit:

$$\phi_{SL} = \underline{(S_2 + S_3)/(S_1 + S_2)} \cdot \varepsilon_{C,CR} / (d_1 \cdot D) \tag{2}$$

The ratio of the depth of neutral axis at the stable limit to the depth of column:

$$x_{n1} = \underline{(S_1 + S_2)/(S_2 + S_3)} \cdot d_1 \tag{3}$$

where, S_1, S_2, and S_3 are the areas shown in Fig. 2,
$\varepsilon_{C,CR}$ is the concrete strain in the extreme compressive fiber at the stable limit as shown in Fig. 2, and
d_1 is a ratio of the distance from the extreme compressive fiber to the tensile steel bars to the column depth.

The drift angle of columns with a shear-span ratio of about 2 is represented by the rotation angle of the hinge region, and the rotation of the hinge region is approximately given by multiplying the curvature at the critical section by the depth of the column, after the hinge region is fully developed (Hiraishi *et al.*, 1990b). Therefore the drift angle of columns at the stable limit is given by Eq. (4).

$$R_{SL} \fallingdotseq \phi_{SL} \cdot D \tag{4}$$

where, R_{SL} is the drift angle of columns at the stable limit.

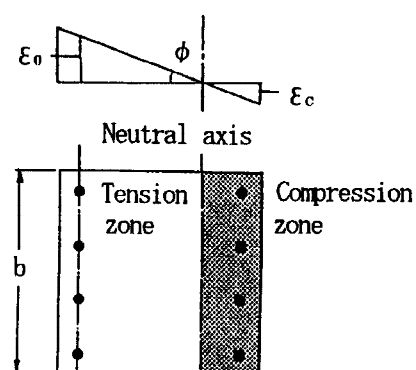

Fig. 1. Symmetrical section.

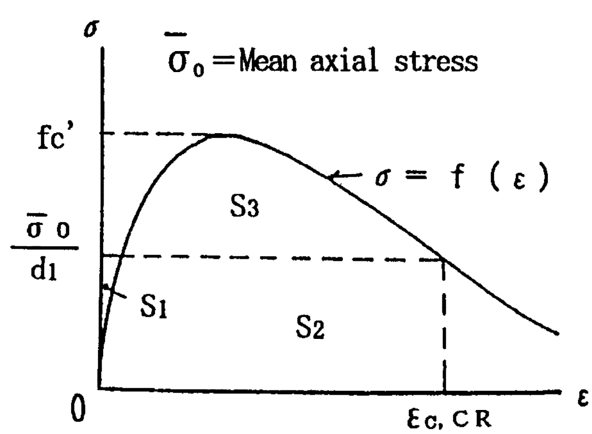

Fig. 2. Assumed stress-strain relation for concrete and axial stress.

DEFORMATION CAPACITY DEFINED BY HYSTERESIS BEHAVIOR OF CONCRETE UNDER CYCLIC LOADING

The deformation capacity is also defined by cyclic loading. This is easily understood by considering the hysteresis characteristic of stress versus strain relations of concrete. Namely, on unloading and reloading in large inelastic strain range, stress of concrete is very small or negligible if it is compared to that at the same strain on the skeleton curve. Therefore, once a whole critical section of columns experiences large inelastic strain in a cyclic loading, the following cyclic loading inevitably forces larger compressive strain in order to sustain the axial load. As a result, the moment resistance of the section decreases and axial shortening starts to occur.

As mentioned above, at least some part of the critical section should be elastic in the cyclic loading, to prevent the axial shortening or cyclic moment deterioration. Therefore, in order to define the deformation capacity under cyclic loading, this condition should be examined at each loading step. However, in the following discussion, it is assumed that while the section is stable after flexural yielding in cyclic loading at a certain deformation amplitude, the inelastic region develops at just both edges of the critical section at both positive and negative peak deformations. On the basis of this assumption, the deformation capacity is obtained by examining the axial load carrying capacity of the critical section at zero deformation, in which inelastic regions have developed at both edges depending on the peak curvature and axial force considered.

DESIGN CHART OF DEFORMATION CAPACITY

Design Chart

Figures 3 and 4 show a core cross section considered and the simplified model of stress versus strain curve of concrete used in the following examples. In Fig. 4, ε_B is the strain at the maximum strength of confined concrete, f_c' is the maximum strength of confined concrete, and α is a descending slope of confined concrete. The cover concrete is neglected because large deformations are considered. Figure 5 shows the relation between the curvature at the stable limit and axial stress ratio; $N/(b'D'f_c')$, where N is the axial force. Figure 6 shows the stress and strain profiles at the two peak curvatures and zero curvature, at the deformation capacity defined by hysteresis behavior of concrete during cyclic loading. The sum of axial stress is the same at these three curvatures, and it is the axial force defining this deformation capacity. The calculated relation between this deformation capacity and axial stress ratio is shown in Fig. 7. Figure 8 shows both results. As seen in Fig. 8, the deformation capacity defined by hysteresis behavior of concrete is dominant.

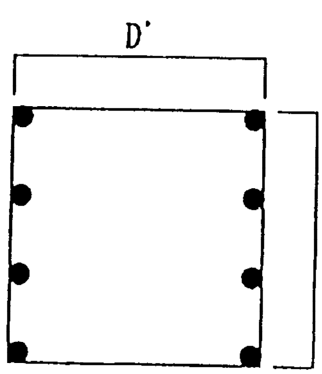

Fig. 3. Core section.

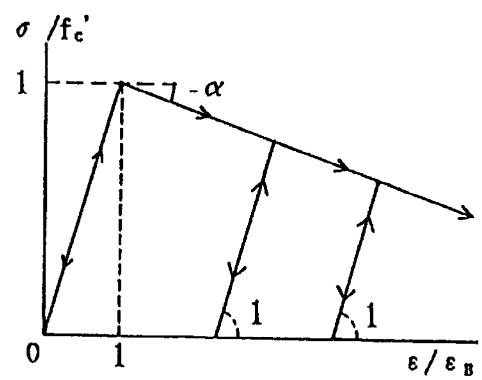

Fig. 4. Simplified stress-strain relation of core concrete.

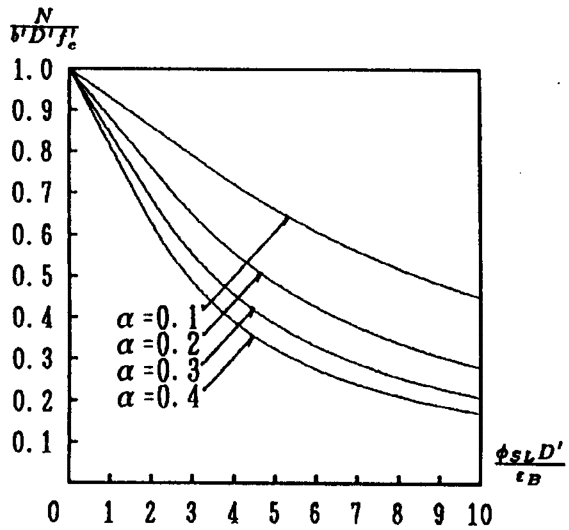

Fig. 5. Deformation capacity defined by stable limit.

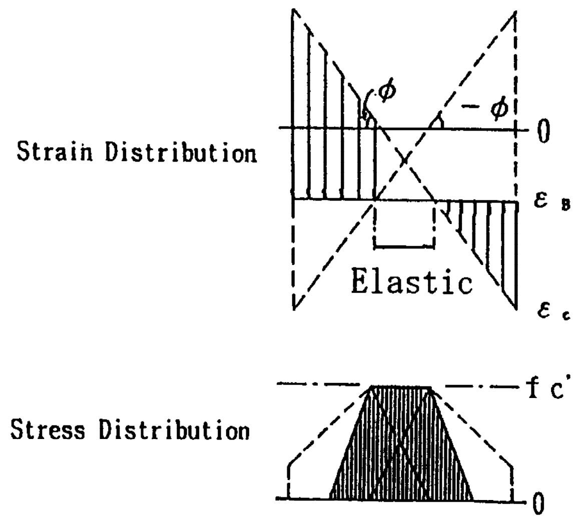

Fig. 6. Strains and stresses at peak and zero curvatures.

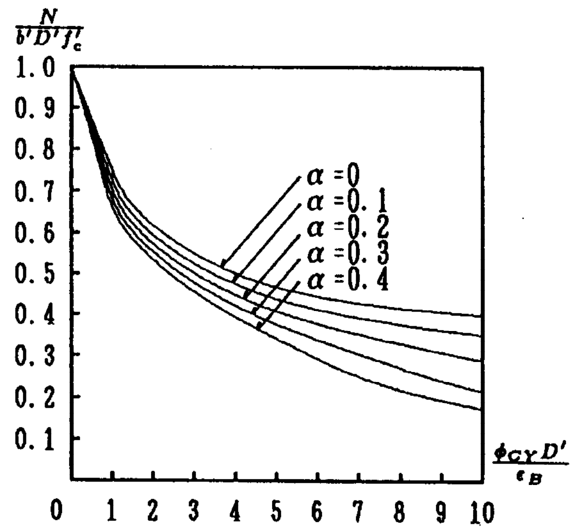

Fig. 7. Deformation capacity defined by hysteresis behavior of concrete.

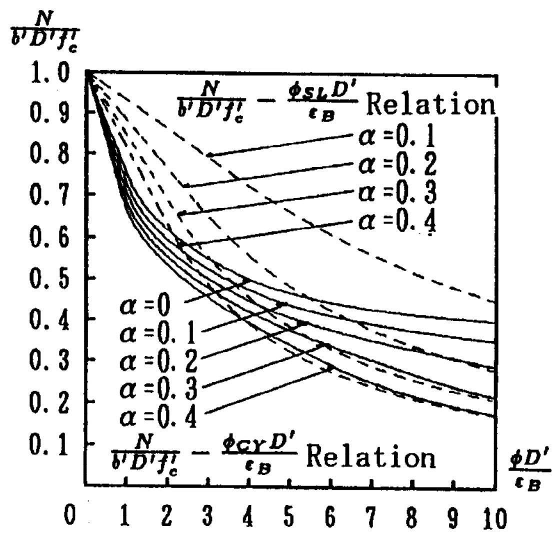

Fig. 8. Deformation capacity of columns under cyclic loading.

Comparison Between Fiber Model Analysis and Design Chart

The results mentioned above are examined in Fig. 9. The stress versus strain curve of core concrete with a constant descending slope of 0.1 of α is used in the fiber model analysis. There are a couple of fiber model analyses with a different axial stress ratio under the same curvature amplitude for cyclic loading: one is judged to be a little greater than the axial stress ratio corresponding deformation capacity and the other is a little less. These results are shown at four different curvatures. All the results of the fiber model analyses with a little smaller axial stress ratio show stable moment versus curvature relations, while those with a little greater ratio show moment deterioration under cyclic loading.

DESIGN EQUATION OF DEFORMATION CAPACITY

Equations 5 and 6 approximately represent the relations with α =0.2 and ε_B =0.4% in Fig. 8 when the drift angle is represented as $R = \phi D'$.

The deformation capacity of columns under monotonically increasing loading:

$$Ru = (1-\eta)/24 \quad \text{for} \quad Ru \leqq 0.03, \quad Ru = (1-2\eta)/14 \quad \text{for } 0.03 < Ru \leqq 0.06 \qquad (5)$$

The deformation capacity of columns under cyclic loading:

$$Ru = (1 - 2\eta) / 14 \quad \text{for} \quad Ru \leqq 0.06 \tag{6}$$

The value of 0.2 of α corresponds to that of the core concrete of columns with the minimum lateral reinforcement (Matsuura *et al.*, 1992). Figure 10 shows the comparison between these equations and the deformation capacities of the experimental results which are assumed to be the deformation at the deterioration in strength of 95% of the ultimate moment. Also the axial stress ratio; η is modified as the following Eqs. (7) and (8), by considering the effect of longitudinal steel bars in the center of the cross section, and f_c' is estimated by the equation proposed by Nakatsuka *et al.*, 1989.

$$\eta = (N - N_d) / (b' D' f_c') \tag{7}$$

$$N_d = a_c \cdot \sigma_y / 2 \tag{8}$$

where, N is the axial force of columns, a_c is the amount of longitudinal steel bars at the center of the cross section of column, and σ_y is yield stress of the steel bars.

It is found that the proposed design equations gave a lower boundary of deformation capacity as expected.

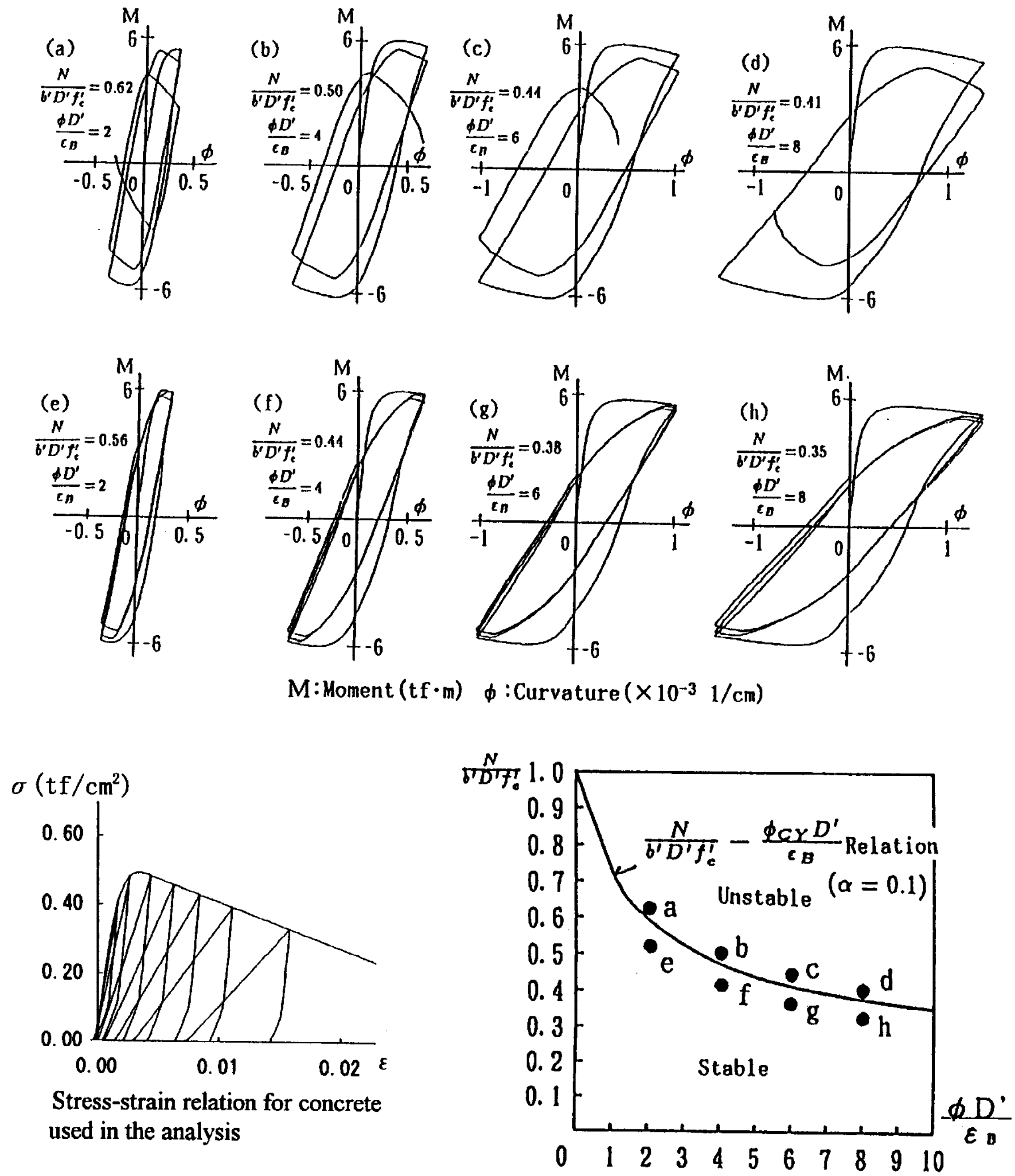

Fig. 9. Examples of fiber model analysis related to deformation capacity.

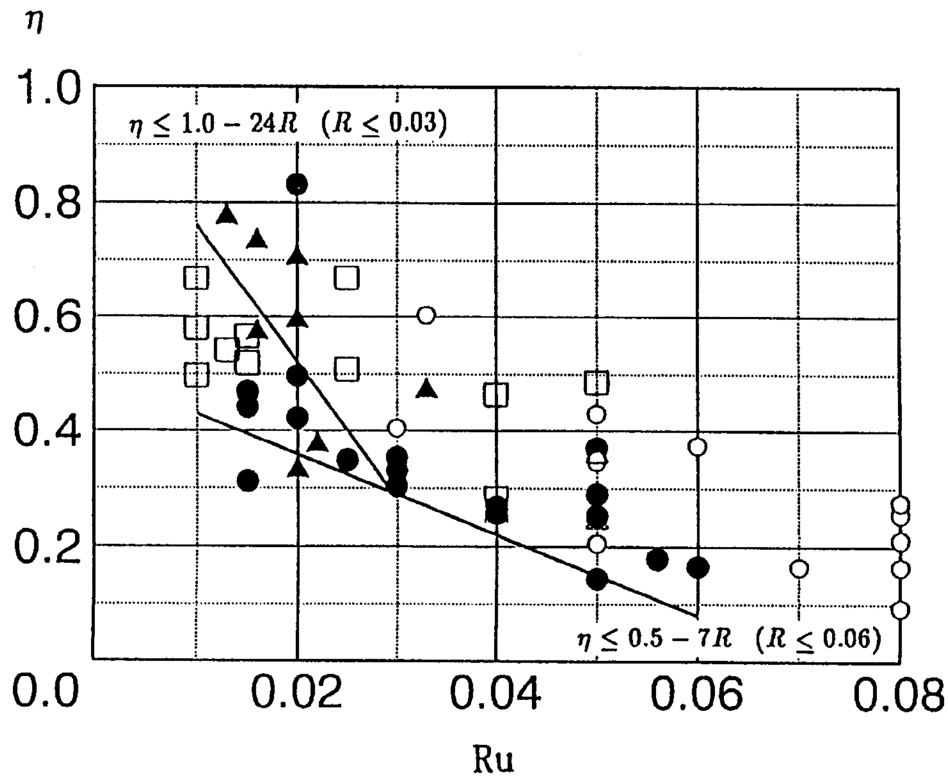

● : Constant axial force, Cyclic loading, Flexural crush failure
○ : Constant axial force, Cyclic loading, Little deterioration
▲ : Varying axial force, Cyclic loading, Flexural crush failure
or Constant axial force, Monotonic loading, Flexural crush failure
△ : Varying axial force, Cyclic loading, Little deterioration
or Constant axial force, Monotonic loading, Little deterioration
□ : Constant axial force, Cyclic loading, Flexural crush failure with vertical cracks

Fig. 10. Experimental relationships between axial stress ratio and deformation capacity of columns and those proposed for seismic design.

CONCLUSIONS

The following conclusions were drawn from this study on deformation capacity of columns subjected to high axial stress.

1)Under cyclic loading, the hysteresis behavior of concrete has a great influence on ductility. The deformation capacity by this is proposed in this paper by considering three deformation stages of the two peak deformations and zero deformation. The smaller of the two being defined by hysteresis behavior of concrete and the stable limit govern the deformation capacity of columns subjected to cyclic loading.

2) The two deformation capacities mentioned above are shown in the charts. Mostly, the deformation capacity defined by hysteresis behavior of concrete is dominant. The proposed chart of deformation capacity shows excellent correlations to fiber model analyses.

3) Finally, this paper proposes the simple structural design equations of the deformation capacity of columns based on theoretical results, and shows the comparison between these and experimental results. The proposed equations provide an excellent lower boundary of the experimental results.

ACKNOWLEDGMENT

The authors would like to express their thanks to Mr. Akira Yagenji at Hazama Corporation for his kind cooperation.

REFERENCES

Hiraishi, H. and E. Inai (1990a). Theoretical Study on Deformation Capacity of R/C Columns Beyond Flexural Yielding. *Journal of Struct. Constr. Engng, Architectural Institute of Japan (AIJ)*, 408, 21-30.

Hiraishi, H., E. Inai, Y. Itakura, T. Takasaki, Y. Ishiwata, T. Kawashima and M. Teshigawara (1990b). Deformation Capacity Beyond Flexural Yielding of Reinforced Concrete Columns Part 1. *Journal of Struct. Constr. Engng, AIJ*, 410, 27-39.

Hiraishi, H., E. Inai and A. Yagenji (1993). Deformation Capacity of Reinforced Concrete Columns under Cyclic Loadings. *Journal of Struct. Constr. Engng, AIJ*, 454, 127-138.

Inai, E. and H. Hiraishi (1992). Deformation Capacity Beyond Flexural Yielding of Reinforced Concrete Columns Part 2. *Journal of Struct. Constr. Engng, AIJ*, 440, 67-76.

Koyanagi, W., K. Rokugo and H. Iwase (1988). Toughness Evaluation and Toughness Design of Reinforced Concrete Beams. *Colloquium on Ductility of Concrete Structures and Its Evaluation, Japan Concrete Institute*, 87-98.

Nakatsuka, T., K. Suzuki and M. Sugata (1989). Mechanism of Confinement and Strength-Deformation Characteristics of Confined Concrete with Rectangular Lateral Reinforcement. *Proceedings of the Japan Concrete Institute*, 11, No. 2, 449-454.

Suzuki, K., T. Nakatsuka and K. Inoue (1988). Ultimate Limit Index Points and their Characteristics of Partially Prestressed Concrete Beam Sections. *Colloquium on Ductility of Concrete Structures and its Evaluation, Japan Concrete Institute*, 193-204.

Matsuura, T. and A. Yagenji (1992). Review of Experimental Studies on RC Columns Subjected to Uniaxial Compressive Load. *Summaries of Technical Papers of Annual Meeting, AIJ, C*, 1005-1006.